euspen's 16th International Conference & Exhibition, Nottingham, UK, May 2016
www.euspen.eu

An integrated measurement method for complex micro-scale geometries

Amir Rabani[1], Nicola Senin[1,2], Franz Helmli[3], Paul Butler-Smith[1,4], Richard Leach[1]

[1]*Advanced Manufacturing Technology Research Group, University of Nottingham, NG7 2RD Nottingham, United Kingdom*
[2]*Department of Engineering, University of Perugia, 06100 Perugia, Italy*
[3]*Alicona Imaging GmbH, Dr.-Auner-Straße 21a - 8074 Raaba, Graz, Austria*
[4]*paul.butler-smith@nottingham.ac.uk*

Abstract
Micro-scale geometries are becoming commonplace in many high-precision manufacturing applications. Micro-drilling processes, for example, are being employed for producing holes in demanding applications involving fluid transfer, atomisers and micro-mechanics. This paper explores the measurement and characterisation of a high aspect-ratio micro-hole (nominal diameter approximately 1000 µm, aspect-ratio 1:10), produced using abrasive waterjet in Ti6Al4V. X-ray computed tomography, contact micro-coordinate metrology and focus-variation microscopy are used for measuring the hole surfaces, and dedicated computational geometry algorithms are applied to obtain critical hole dimensions, such as radius as a function of depth. The comparison of the measurement and characterisation results obtained by means of the different solutions explored hints at new approaches for multisensor data fusion that can help reduce bias in the measurement of high aspect-ratio micro-scale features.

High aspect-ratio micro-scale holes, coordinate metrology, multi-sensor data fusion

1. Introduction

The production of micro-scale geometries to defined tolerances has facilitated the advancement of numerous complex systems to satisfy demanding industrial requirements. High aspect-ratio micro-scale geometries, where lengths are larger than widths by an order of five or more, have been used in many applications [1-6], high aspect-ratio, micro-scale holes playing a dominant role. There are various methods for fabricating high aspect-ratio micro-scale holes [7-11]. Abrasive waterjet machining (AWJM) is a popular one; it is non-contact and has virtually no thermal influence on the workpiece, and due to its high versatility to process any material, it has multi-axes operation and negligible cutting forces [12]. Quality control of high aspect-ratio, micro-scale holes is still a challenge because it is difficult to measure such structures by using existing measurement technologies. Contact based technologies (i.e. micro-CMMs) have accessibility problems and are limited on the amount of points that can be acquired in a reasonable time. Optical profilometers have the benefit of higher point cloud densities and higher acquisition speeds, but are also limited by the narrow spacing between walls (reducing the amount of usable light reflected back into the detector) and by measurement being intrinsically unidirectional (the specimen must be tilted to acquire vertical or high-sloped walls). X-ray computed tomography (XCT) is most likely the only technology which can image a high aspect-ratio, micro-scale feature such as a micro-hole in one measurement process. However, XCT is still significantly limited by resolution and accuracy issues [13]. The demand for metrological information related to micro-scale features is constantly increasing and is pushing the boundaries of current measurement technologies. Competitive advantage in metrology for quality inspection can be gained by working on improving the metrological performance of the existing techniques, and by developing novel multi-sensor data fusion approaches that combine results ultimately overcoming the limitations of each single sensor [14].In this paper, a high aspect-ratio micro-hole fabricated via abrasive waterjet cutting is measured with XCT, focus variation (FV) microscopy and contact CMM. The acquired datasets are processed through a dedicated, algorithmic characterisation pipeline aimed at assessing hole diameter as a function of depth. The results from the different measurement methods are compared and a method is proposed to reduce bias in the XCT and focus variation results, based on assuming CMM data as the "true" reference. CMM uncertainty is neglected to simplify fusion; which holds as long as CMM uncertainty is smaller than FV and XCT uncertainties. Further work is in progress on fusion models incorporating CMM uncertainty.

2. Materials and methods

The test case consists of a through-hole of nominal 1 mm diameter realised in a Ti6Al4V plate of approximately 10 mm thickness by abrasive waterjet machining (AWJM). The aspect ratio is approximately 1:10. The hole shape is typical of the AWJM process, with a smaller entry and a larger exit section. Details of how the hole was measured are provided in the following sections.

2.1. X-ray computed micro-tomography

A Zeiss XRADIA XCT system Versa XRM-500 was used. The specimen was imaged resulting in 1004 RGB JPEG images (slices) each of size 1024×1004 pixels, voxel size 13.5 µm and voxel intensity encoded in 256 levels. This configuration allowed the hole topography to be measured in its entirety and all in one process. The hole isosurfaces (*XCT dataset*) were extracted with the 50 % intensity threshold rule [13] with no mesh simplification/smoothing. A close-up view of the hole entry region is illustrated in Figure 1.a.

2.2. Focus variation microscope

An Alicona Infinite Focus G5 focus variation microscope (FV), with Real3D rotation unit and 20× objective was used. The hole was imaged at the entry and exit sides, with part refixturing in

between. The specimen was mounted onto a computer-controlled tiltable fixture (the Real3D rotation unit) in order to acquire the high-sloped/undercut surfaces: multiple datasets were acquired at different orientations, and stitched together using FV software. The final datasets, one for the entry and one for the exit surface, were provided as triangulated models (*FV datasets*). The entry region is shown in Figure 1.b. The microscope was operated at 50 nm vertical resolution, and 5.5 µm – 5.8 µm point spacing. Due to the high aspect-ratio, it was not possible to image the entire topography of the internal surfaces; however, a more detailed topography with respect to XCT data was returned (compare Figure 1.a and Figure 1.b).

2.3. Contact CMM

A Mitutoyo Euro-C-A121210, with RENISHAW Low Force Module: TP200LFMOD+TP200 and RENISHAW Stylus Probe: A-5003-1345 DU/AR was used (tip radius: 0.5 mm). The hole was accessed from the entry and exit sides, with part refixturing in-between. At each side, four points were taken to identify the entry/exit surface and align it to the z = 0 plane; then, sets of thirty-six points were taken along circumferential paths with constant depth spacing of 0.5 mm on the hole internal surfaces (*CMM datasets*). In Figure 1.c, the CMM points for the hole entry region are shown. Low point density and comparably large stylus tip radius filter out high-frequency topography details.

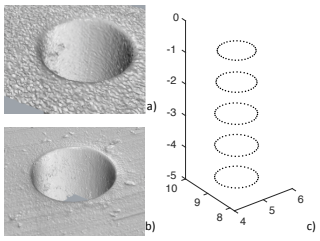

Figure 1. Close-up views of the hole entry side; a) XCT triangulated model; b) FV triangulated model; c) CMM point set (units are in mm).

2.4. Data analysis process

The analysis focused on investigating how the hole cross-section varies with depth. The following process was applied to the FV and XCT datasets (both triangulated models) and was repeated separately for the entry and exit sides: algorithmic segmentation of the dataset to identify the hole support surface (the region surrounding the hole); alignment of the support surface to the *xy* plane; hole cross-sectioning with 2 µm vertical spacing; least-squares robust fitting to a circle of each cross-section; extraction of circle centre and radius. As an example, cross-sections and fitted circles for the FV dataset (entry side) are shown in Figure 2.

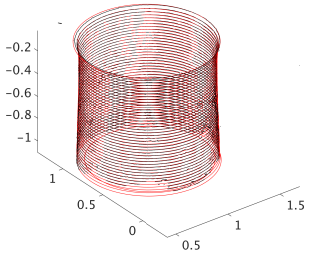

Figure 2. Cross-sections (black) and fitted circles (red) for the FV dataset (entry side). Units in mm.

For the CMM datasets, it was possible to do circle fitting directly onto each set of thirty-six points (i.e. no need for cross-sectioning).

3. Results

Plots of the radii as a function of depth are shown in Figure 3 for the hole entry region, for the XCT, FV and CMM datasets. The plots refer to the 0.5 mm to 1.2 mm depth interval, i.e. from the first available CMM radius to the depth after which the FV radius degenerates, as there are not enough measured points to achieve a reliable circle fitting.

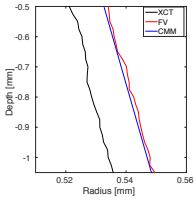

Figure 3. Plots of the radiuses as a function of depth at the hole entry side; R_{XCT} (black), R_{FV} (red), R_{CMM} (blue). Axes proportions are altered.

Disagreement between radii was computed as signed pairwise differences (i.e. error), again as a function of depth. The results for the entry side (mean ± st.dev) were: $E_{FV\text{-}CMM}$ = R_{FV}-R_{CMM} = 0.93 µm ± 0.39 µm; $E_{XCT\text{-}CMM}$ = R_{XCT}-R_{CMM} = -9.49 µm ± 1.02 µm. Similar results were obtained for the hole exit side: $E_{FV\text{-}CMM}$ = 2.81 µm ± 0.73 µm; $E_{XCT\text{-}CMM}$ = -7.95 µm ± 0.78 µm. The large deviation of XCT results with respect to FV and CMM is due to sensitivity to isosurface extraction, one of the key challenges of XCT measurement [13]. With d the depth coordinate of the hole, and assuming the function $R_{CMM}(d)$ as representative of the true radius (as per the assumptions discussed in the introduction), local bias of the functions $R_{XCT}(d)$ and $R_{FV}(d)$ can be reduced by simply subtracting the local error value at each depth; thus yielding the bias-reduced functions: $R'_{XCT}(d)$= $R_{XCT}(d)$ - $E_{XCT\text{-}CMM}(d)$ and $R'_{FV}(d)$= $R_{FV}(d)$ – $E_{FV\text{-}CMM}(d)$. Local bias cannot be completely eliminated since $R_{XCT}(d)$ and $R_{FV}(d)$ contain also a random error component that cannot be isolated without replicate measurements.

4. Conclusions

A high aspect-ratio micro-hole was measured with XCT, FV and contact CMM. Radius as a function of depth was obtained algorithmically from all the three datasets. XCT featured the most complete coverage of the hole, but also the largest bias against the CMM results, assumed as true. FV captured the most topographic detail at higher frequencies. It was shown that it is possible to reduce bias in the FV and XCT radii by using the CMM results as a correction factor. These findings pave the way for future work on multi-sensor data fusion solutions where a small number of sparse CMM data points can act as attractors to correct much denser and information-richer point sets, such as those obtainable via FV and XCT.

References

[1] Kao C C and Shih A J 2007 *Meas. Sci. Technol.* **18** 11 3603
[2] Masuzawa T, Hamasaki Y and Fujino M 1993 *CIRP Annals-Mfg. Tech.* **42** 1 589-592
[3] Allen D M and Lecheheb A 1996 *J. Mater. Process. Tech*. **58** 1 53-66
[4] Lu Y and Chen S C 2004 *Adv. Drug. Del. Rev.* **56** 11 1621-1633
[5]Peiner E, Balke M and Doering L 2009 *Microelect. Eng*. **86** 4 984-986
[6] Garbini J L, Saunders R A and Jorgensen J E 1991 *Prec. Eng.* **13** 2 125-134
[7] Vestavik O M and Skaugen E 1992 *Jet Cut. Tech.* **13** 389-402
[8] Masuzawa T, Tsukamoto J and Fujino M 1989 *CIRP Annals-Mfg. Tech.* **38** 1 195-198
[9] Tunna L, O'Neill W and Sutcliffe C 2005 *Opt. Laser Eng.* **43** 9 937-950
[10] Sen M and Han H S 2005 *Int. J. Mach. Tool Mfg*. **45** 2 137-152
[11] Iwata K, Moriwaki T and Hoshi T 1981 *CIRP Annals-Mfg. Tech*. **30** 1 27-30
[12] Rabani A, Marinescu I and Axinte D 2012 *Int. J. Mach. Tool Mfg.* **61** 80-89
[13] Kruth J P, Bartscher M, Carmignato S, *et al*. 2011 *CIRP Annals-Mfg. Tech.* **60** 2 821-842
[14] Wang J, Leach R K Jian X 2015 *Surf. Top: Met. Prop.* **3** 2